Control of a Transitioning Boundary Layer using Surface-Mounted Electro Active Polymers

Tyler Van Buren and Michael Amitay[1],*

Mechanical, Aerospace and Nuclear Engineering Department,
Rensselaer Polytechnic Institute, Troy, NY 12180, USA

ABSTRACT

Micro air vehicles (MAV) are a major focus of aerodynamics today with many military as well as civilian applications. MAV flight is dominated by the unsteady characteristics of low Reynolds number flows. Three-dimensional separations may occur at random on different parts of the wing, causing highly unsteady forces and moments, as well as full wing stall. In the present work an Electro-Active Polymer (EAP) actuator was examined as a feasible flow control actuator with application to low Reynolds number flows. The performance of the EAP was evaluated using a laser displacement device, where the displacements generated under selected driving frequencies and input voltages were recorded. It was shown that the deflections could reach up to 0.35 mm at frequencies below 40 Hz. The surface deflection was found to be parabolic across the span and width of the actuator. Hot-wire anemometry measurements were conducted on a flat plate equipped with a trailing edge flap in a low Reynolds number wind tunnel to study the effects of the EAP on a transitional boundary layer. Two actuation frequencies were chosen, corresponding to the Tollmien-Schlichting waves of the boundary layer and the Kelvin-Helmholtz waves (due to the presence of an inflection point). The actuation at a frequency corresponding to the inflection point was found to be the most effective in altering the boundary layer as well as its turbulence intensities.

1. INTRODUCTION

1.1. Micro Air Vehicle Flight

At low Reynolds numbers the flow is dominated by viscosity, and thus more susceptive to separation. MAVs can experience flow separation due to varying flow conditions such as gusts and turbulence that can induce laminar separation bubbles (LSB) on the wings, as was shown by Bastedo and Mueller (1986). Figure 1 shows an artistic representation of a 3-D separation bubble over an airfoil at a low Reynolds number (Winklemann and Barlow, 1980). Given that MAVs are a relatively new technology it is important to fully understand the flow field at this low range of Reynolds numbers and address the issue of separation bubbles using an advanced active flow control technique, which is the motivation of the present work.

Flow control has been a rising field in fluid dynamics over the last few decades with a wide variety of techniques in aerodynamics alone. A boundary layer naturally undergoes a transition during its development from a laminar (relatively small height, small amounts of momentum near the surface, and low velocity fluctuations) to a turbulent state (larger height, large amounts of momentum near the surface, high velocity fluctuations), and this transition can be controlled by both the pressure gradient and the magnitude of disturbance in the flow field. The two types of boundary layer flow control that dominate the field are laminar flow control, which prevent flow transition to turbulence (i.e., keep a laminar flow), or using flow control to induce turbulence and transition, which can prevent separations. Techniques of laminar flow control range from wing shaping using flaps and leading edge mechanisms to suction on the wing surface. Mueller et al. (2003) reviewed the problems with MAV flight that must be addressed to advance the technology. A significant portion of problems with MAVs is contributed to laminar separation. At Reynolds numbers below 70,000 the authors reported that when laminar separation occurs (often due to gusts) the flow does not transition from laminar to turbulence, for reattachment on the wing and thus
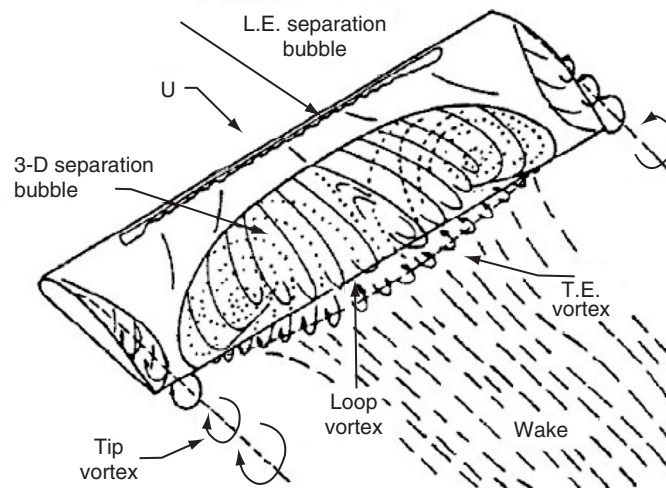
---

*Corresponding author, Email: amitam@rpi.edu

Figure 1. Artistic representation of 3-D separation over an airfoil at low Reynolds number
(Winklemann and Barlow, 1980).

causing full stall. For Reynolds numbers from 70,000–200,000, laminar separation often reattaches on the airfoil causing laminar separation bubbles, which can still pose problems to flight performance due to parasitic drag of the LSB and the unsteady lift associated with it. This motivates the need for an active flow control device that promotes earlier transition and thus reduces the negative effects of laminar separation.

The ability to change the shape of a surface has been shown to significantly affect flow fields on large scales. Pinkerton and Moses (1997) studied the feasibility of using a special high displacement piezoelectric actuator designed at NASA (THUNDER actuator) as a shape altering mechanism on a subscale airfoil. The goal of the research was to show that the actuator was successful in significantly changing the camber under multiple wind tunnel velocities, which extended the region of attached flow over the airfoil at angles of attack above 2 degrees. They found that actuation successfully altered the wing camber with multiple parameters affecting the actuator displacement: magnitude of the applied voltage, tunnel velocity, the angle of attack, and creep and hysteresis of the wafer. Ehlers and Weisshaar (1993) studied the ability of piezoelectric actuators in changing lift characteristics of swept and unswept wings by changing the wings aeroelastic stiffness. Feedback control sensed wing root strains and adjusted active actuator layers to proportionally change wing lift. They found that although lift was successfully adjusted, the effectiveness of the actuator is strongly constrained by the stiffness of the piezo material as well as the implementation of the device on the wing.

Ifju et al. (2002) investigated the development of flexible-wing-based MAV technology to reduce the negative effects of gust conditions. They demonstrated flexible wing concepts on wingspans from 5" to 18" reporting the flexible wing design, fabrication methods, as well as flight data analysis. Through pilot reports and video recordings they reported much smoother flight conditions for a variety of test vehicles.

In recent years Electro Active Polymers (EAPs) have been shown to be a simple solution to surface modification. The EAPs not only provide means to static modification with a constant DC voltage input, but also the means of dynamically altering the surface and thus adding disturbances to the flow for the purpose of promoting early transition. Figure 2 represents a possible implementation of EAPs on an MAV to either promote transition or maintain a laminar flow. Dearing et al. (2007) used EAPs as a means to produce an active dimple to induce controlled vorticity into the flow field. They analyzed the effect of a single actuated dimple with a flow field using PIV and flow visualizations. They reported that a smooth dimple generates vorticity in phase with the dimple motion and the strength of vorticity is proportional to the dimple displacement.

1.2. Flow Control of Laminar Boundary Layers
Understanding the effect of flow control on laminar boundary layers under an adverse pressure gradient is crucial in the choice and application of the flow control device. Marxen et al. (2006) took an in depth look into the control of a laminar separation bubble (LSB) based on linear stability theory. They found that there are frequencies that can be used to excite the flow to reduce the size of a LSB and discussed
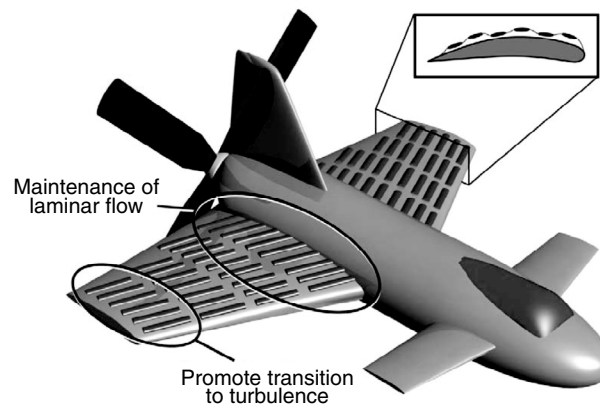
Figure 2. Representation of an EAP implementation on a MAV with wing cross-section depicting a possible deflection of the EAP.

how the size of the bubble affects stability. The authors stated that for larger bubbles the region of instability is larger and the most amplified frequency, the frequency with the highest growth rate, increases. They also found that separation bubbles and wake dynamics could be decoupled and studied independently. Diwan and Ramesh (2007) discussed the effect that infinitesimal and finite disturbances, created by a loudspeaker, on the separation bubble. They showed that finite amplitude forcing caused the bubble to reduce in size, and even infinitesimally small disturbances could control the size of the bubble. Marxen et al. (2003) looked at the transition to turbulence inside a LSB followed by a reattachment using experimental and numerical techniques. The evolution of small disturbances, corresponding to Tollmien-Schlichting waves, was analyzed along with their role in the breakdown to turbulence. This study was extended by Lang et al. (2004) using stereoscopic Particle Image Velocimetry (PIV) and Laser Doppler Anemometry (LDA) to analyze the transition mechanisms in laminar boundary layer separations. They found that the 2D TS waves were the main factor in determining the size and position of the LSB, and the disturbances in the streamwise direction only played a minor role in the transition process.

Abdullah et al., (2009) explored the feasibility of using shape memory alloys as a flexible skin for variable camber airfoils. A shape shifting airfoil possesses many benefits in flight, allowing the optimization of lift-to-drag ratios for all flight conditions. Udovidchik and Morrison (2006) investigated the effects of surface-mounted unsteady dimple on laminar and turbulent boundary layers. The dimples were placed along the span of a cylinder and the separation location for different actuation frequencies was analyzed. They showed that in the vicinity of the dimples, actuated at 10 Hz, the cylinder separation was delayed mainly due to the production of streamwise vortex pairs, which has been seen to prevent separation in numerous works (e.g., Amitay et al., 2001).

Goksel (2007) conducted an in depth study of the effect of plasma-based flow control at low Reynolds numbers (20,000 < Re < 140,000). He found that utilizing plasma-based flow control on an Eppler E338 airfoil significantly increased the lift characteristics of the airfoil. They also showed that using a modulated waveform, with various duty cycles, was still effective in separation control, even for duty cycles as low as 0.66%.

The motivation of the present work is to explore the feasibility of EAP-based flow control to alter the mean and fluctuating velocities of a transitional boundary layer over a flat plate. Utilizing an EAP actuator in a transitional boundary layer, with multiple input voltage conditions to the EAP, the effectiveness of the actuator on the surrounding flow field will be explored. The most effective input conditions to the actuator with respect the boundary layer control will be determined and analyzed, and a conclusion on whether an EAP can be an effective flow control device will be made.

2. EXPERIMENTAL SETUP

The experiments were conducted in a small-scale open-return low Reynolds number blow-down wind tunnel. The operating speed range of the tunnel is between 0.5 m/s to 30 m/s with less than 0.5% free stream turbulence over the velocity range. The test section dimensions are a 10.16 cm × 10.16 cm cross-section and a length of 60.96 cm.

A special flat plate (with an overall length of 0.44 m) was designed to house the EAPs and to test their effect on the boundary layer. The flat plate was instrumented with an adjustable flap (50.8 mm in length) that was installed at the trailing edge of the plate as shown in Figure 3. The flap deflection (with a range of a range of ± 45° and an accuracy of 0.1°) was controlled by a Penn Engineering stepper motor coupled with a US Digital encoder and was used to control the streamwise pressure gradient in the tunnel, seen in Figure 4. The main portion of the flat plate was constructed from aluminum and it was 0.38 m in length (not including leading edge and flap), 0.1 m wide, and 6.35 mm thick. The leading edge of the plate has an elliptical shape (3:1 axes ratio) to minimize local flow separation at the leading edge (Narasimha and Prasad, 1994), and was made from stereolithography (SLA). In addition, the plate incorporated 13 static pressure ports along its centerline, spaced every 25 mm starting 75 mm from the leading edge, in order to quantify the streamwise pressure gradient. The pressure was measured using a Setra differential pressure transducer with a range of 0–0.5" water column and accurate to 0.5% full scale. The pressure was sampled for 60s at 100 Hz, yielding an average of 6×10^3 points.

In the present work, the EAP consisted of five layers, as shown in Figure 5, where the first and third layers served as insulators of the carbon sheet (where the positive charge is applied), the fourth layer is a non-conductive plastic determining the shape of deflection, and the fifth layer is an aluminum plate where the negative charge is connected. When a potential field was applied between the carbon sheet and the aluminum substrate, the carbon sheet was attracted to the aluminum plate and was recessed into the opening of the plastic layer. Note that in the present work the entire surface of the EAP was deflected. The EAP patch was 33.5 mm × 52 mm in size and was installed into the plate (using a plug piece) where its upstream edge was 15.8 mm from the leading edge.
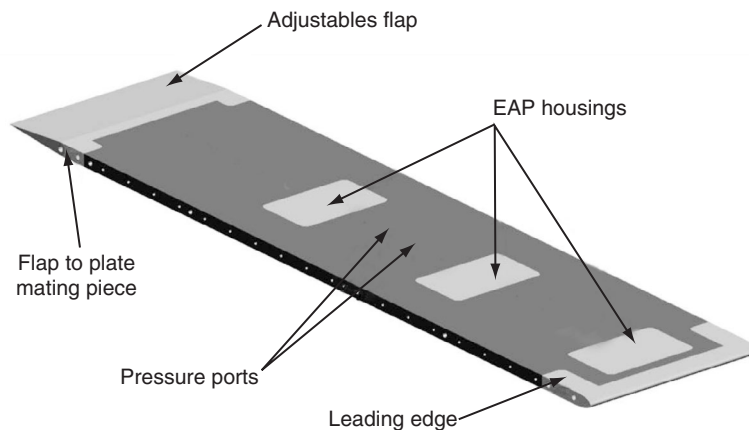

Figure 3. CAD model of the flat plate. Dark grey represents aluminum, light grey represents SLA. Flow is from bottom right to upper left.

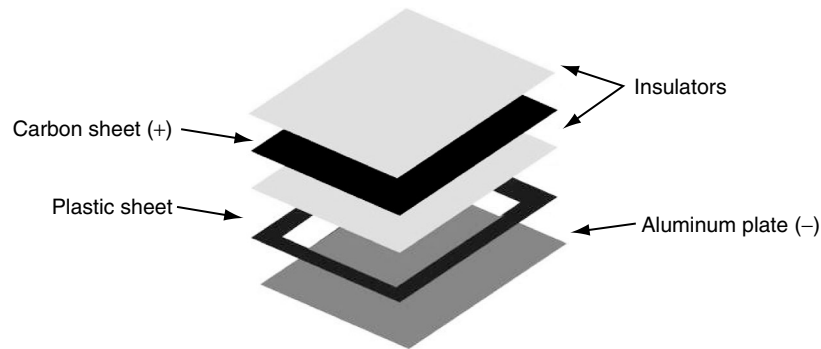Figure 4. The flat plate flap with a stepper motor control.

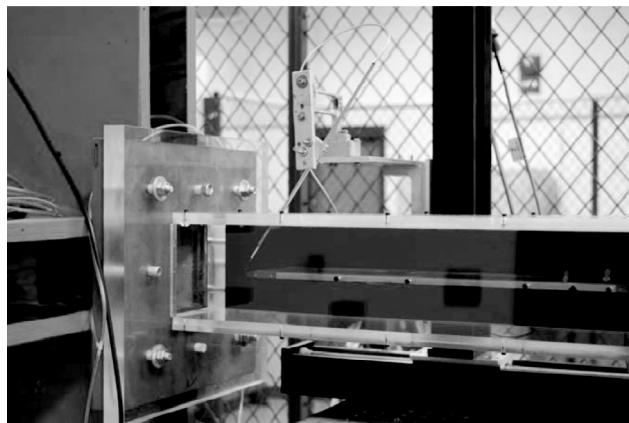Figure 5. EAP layer configuration, artistic representation.

Figure 6. View of the hotwire probe in the test section equipped with the flat plate.

The boundary layer profiles were measured using a single hotwire sensor, via an A.A. Lab Systems LTD (model AN-1005) anemometry. The hotwire was installed in a test section with specially designed brushes to allow it to move in the streamwise direction along the centerline, as well as being able to traverse normal to the plate. The motion was provided by two traverses, which allowed for precise boundary layer measurements to be made close to the wall, see Figure 6. The probe was angled 45 degrees to the plate to minimize the intrusiveness of the probe with the flow measurements. Data were taken at 50 kHz for 30s, yielding an average of 1.5×10^6 points.

3. RESULTS
3.1. EAP Calibration
Before investigating the effect of the EAPs on the flow over the flat plate it was important to quantify their performance (e.g., driving frequencies, input voltages, surface displacements, etc.). The EAPs are unique in a sense that the displacement frequency of the EAP is twice the driving frequency because the EAP deflects when a potential difference is present (the EAP surface is attracted by a change in voltage, both from negative to positive and vice versa). A Trek Model 609E-6 amplifier was used, coupled with an in-house LabView program (a wave signal generator), to drive the EAPs at up to voltage amplitude of 2000 V and driving frequencies up to 500 Hz. A *Polytec: PDV 100* Laser Doppler Velocimetry (LDV) system was used to measure the velocity of the surface deflection, and by knowing the initial location of the EAP surface, the displacement profile was obtained. The LDV was attached to a three-axis traverse system providing the ability to record the deflection of the EAP with a spatial resolution of 127 μm. A picture of the experimental setup is presented in Figure 7. Data were taken every 3 mm in both the x and y directions to quantify the EAP surface deflection.

Figures 8 and 9 show the phase averaged, peak surface deflection of the EAP, driven at two frequencies of 40 Hz and 500 Hz and at a voltage of 2000 V. Note that these frequencies are associated
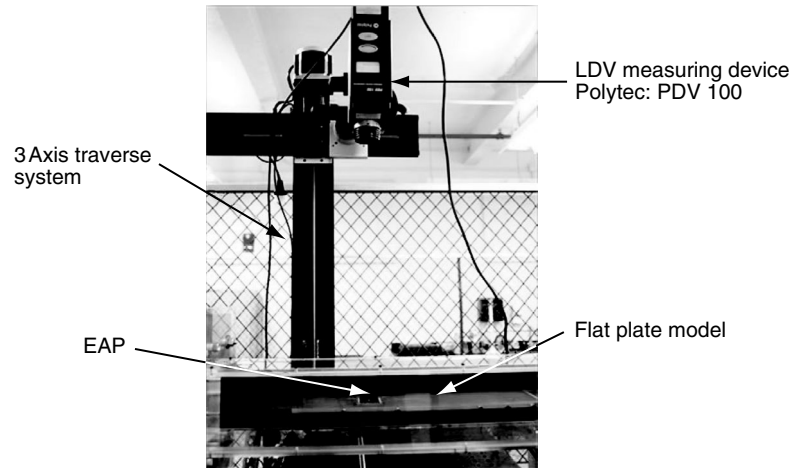
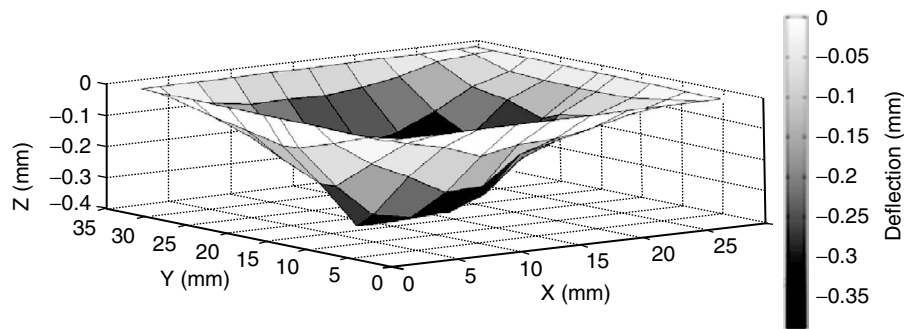Figure 7. LDV setup for EAP calibration experiments.

Figure 8. 3-D surface deflection at actuation frequency of 40 Hz and a voltage amplitude of 2000 V.
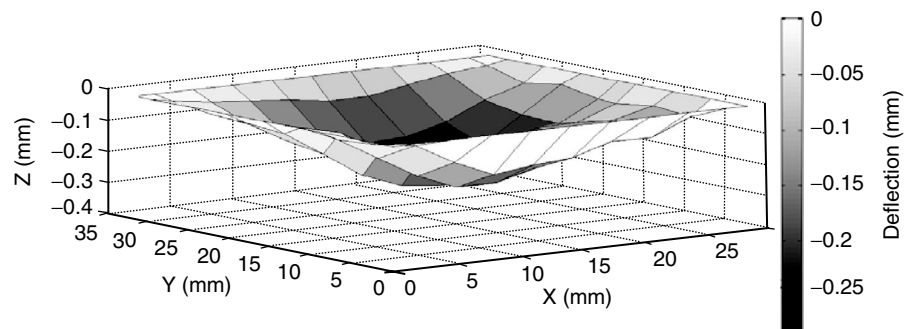

Figure 9. 3-D surface deflection at an actuation frequency of 500 Hz and a voltage amplitude of 2000 V.

with the boundary layer TS wave and the point of inflection's Kelvin-Helmholtz wave, respectively. The EAP's deflection is relatively large (~35% of the local boundary layer height), providing up to 0.35 mm peak displacement magnitude. With these displacements it was assumed (and proven, as will be shown later) that these EAPs would be affective in altering the boundary layer. It is important to note that the EAP calibration was conducted in the presence of the cross-flow (5 m/s) to ensure that the deflection measurements accommodated the shear stresses induced by the cross-flow.

3.2. Boundary Layer Measurements
3.2.1. Baseline
Following the quantification of the EAP, boundary layer measurements were conducted using a single hotwire. In the present experiments, flap angles of 0° and 12° were chosen and a free stream velocity of 5 m/s is used throughout. The 0° flap angle was chosen to show that the flat plate boundary layer fits to the Blasius boundary layer solution (Schlichting, 1979) at streamwise locations prior to the transition to a turbulent boundary layer. The 12° flap angle was chosen such that it induced a less favorable pressure gradient.

Figure 10 shows the pressure coefficient variation in downstream distance along the centerline of the flat plate when the flap is deflected to either 0° or 12°, from which the pressure gradient can be deduced. As expected, the deflection of the flap causes a reduction in the pressure gradient. To quantify the incoming boundary layer at both angles it was helpful to compare them to the theoretical laminar solutions. Figure 11 presents a comparison between the Blasius solution and the measured boundary layer at a streamwise location of 165 mm (from the leading edge) with a flap angle of 0°. As can be seen, the measured boundary layer compares quite well to the Blasius theoretical prediction, suggesting that the boundary layer is laminar. Figure 12 presents the measured boundary layer profile at the same streamwise location but for a flap angle of 12° and is compared to the Blasius solution. Clearly, the agreement of the measured data with the theoretical profile is not as good as the 0° flap angle case, suggesting that the flow field is most likely transitional at that streamwise location, which is due to the reduction in the pressure gradient (a reduction in favorable pressure gradient causes the boundary layer to transition earlier).

To better compare the 0° flap deflection boundary layer to the 12°, the velocity profiles were measured at several locations: 165 mm, 203 mm, 241 mm, and 305 mm from the plate's leading edge. This provided a good indication of the boundary layer development for both cases as well as revealed the streamwise domain along the plate that exhibited an inflection point in the boundary layer profile. Figure 13 presents the velocity profiles at the different streamwise locations (note that for each profile, the zero velocity was adjusted to represent the dimensional distance from the leading. It can be seen that deflecting the flap downwards significantly changes the boundary layer profile. At the first downstream location, when the flap is deflected to 12° the boundary layer is pulled down towards the surface. Farther downstream, at x = 203 mm and 241 mm, an inflection point is clearly visible, suggesting that the flow at a flap deflection of 12° has started to transition to a turbulent boundary layer farther upstream on the flat plate (compared to the 0° case) due to the reduced pressure gradient. Farther downstream, at 305 mm, the boundary layer is fuller and has more momentum near the surface than that of the 0° flap angle case, which is indicative of transitional flow.
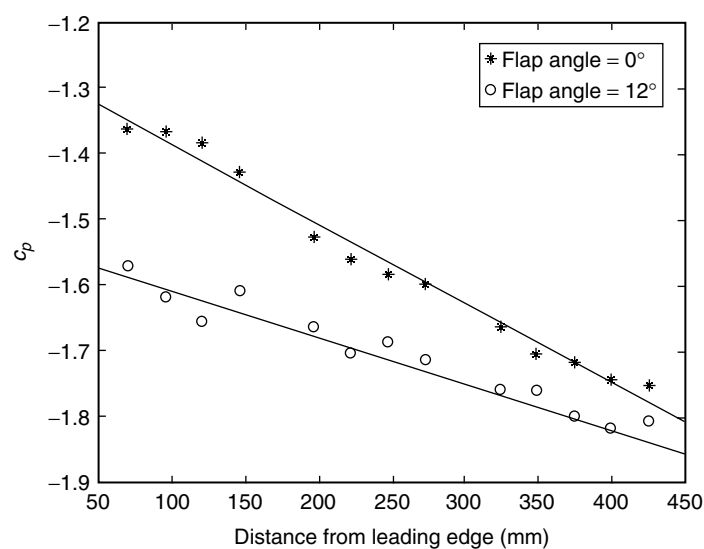

Figure 10. Pressure gradient along the centerline of the flat plate at two flap deflections.
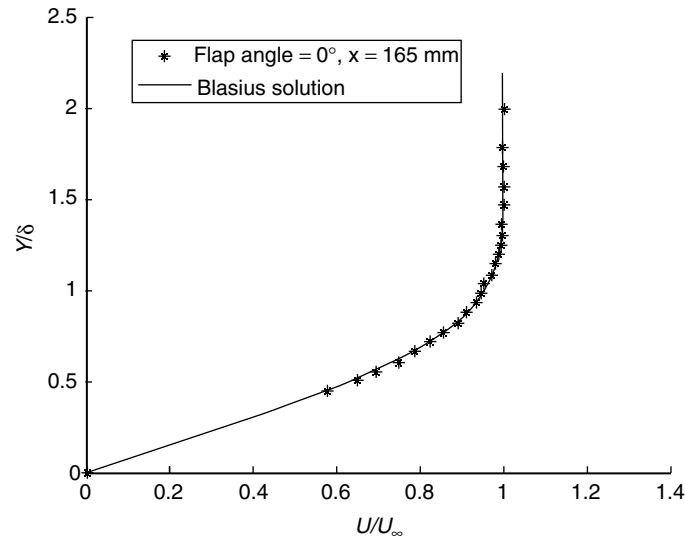
Figure 11. Measured boundary layer compared to the Blasius solution at a streamwise
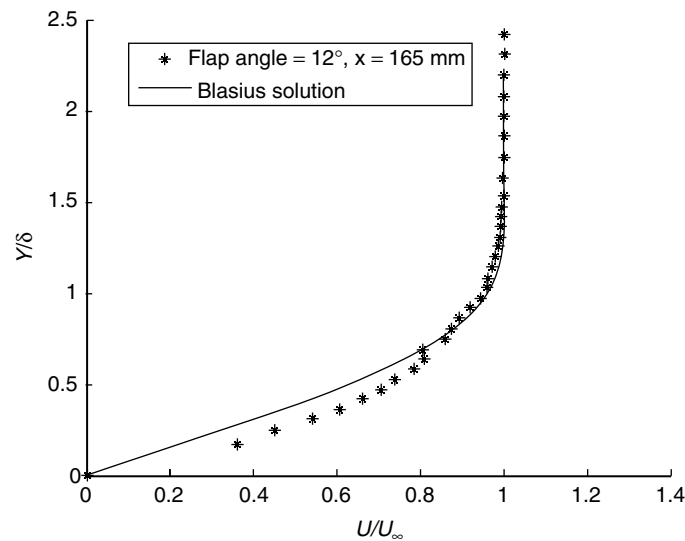location of 165 mm, and a flap deflection of 0°.

Figure 12. Measured boundary layer compared to the Blasius solution at a streamwise
location 165 mm, and a flap deflection of 12°.

The feasibility of the EAPs to alter the flow field was examined for the case where the flap deflection was 12° flap, due to the presence of the inflection point, which makes the transitional boundary layer more susceptible to the application of flow control. Boundary layer measurements were taken at higher spatial resolution near the streamwise location where the inflection point was present in the boundary layer profile. Figure 14 presents the boundary layer at 19 mm, 63 mm, 114 mm, 165 mm, 190 mm, 203 mm, 216 mm, 228 mm, 241 mm, and 305 mm, with a line representing the boundary layer thickness (defined at the location where the local velocity equals 95% of free-stream velocity). Near the leading edge (at x = 19 mm, just downstream of the elliptical leading edge) the boundary layer is still developing, whereas between x = 63 mm and 165 mm the boundary layer resembles a laminar boundary layer and compares well with the Blasius solution as was shown above. As the flow transitions to a turbulent boundary layer its thickness increases drastically with downstream distance. Furthermore, the boundary layer profiles between x = 190 mm to 241 mm exhibit an inflection point.
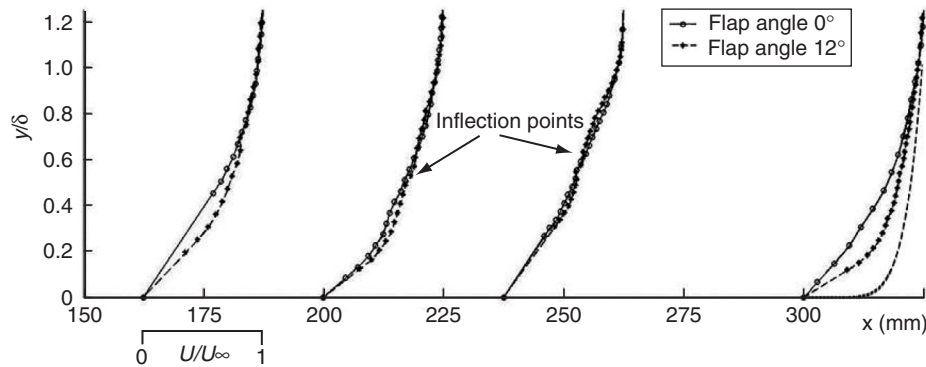
Figure 13. Normalized boundary layer profiles offset by their streamwise location from the plate leading edge for two flap deflections: 0° and 12°. Turbulent boundary layer 1/7th power law also plotted (--) for reference at final location.
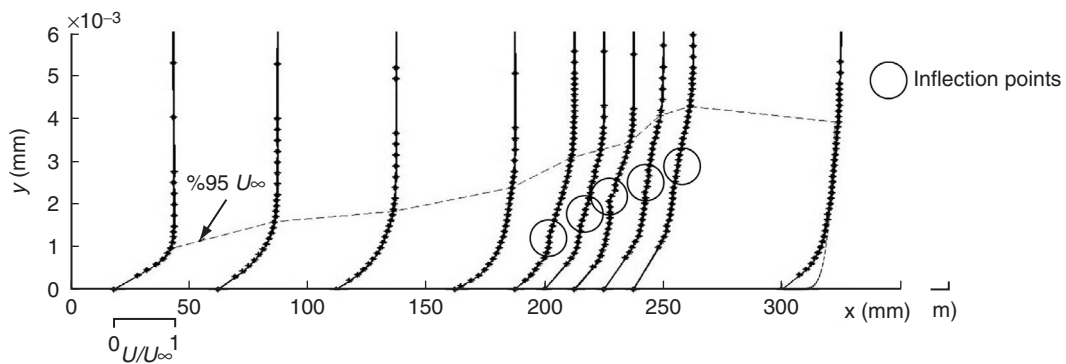

Figure 14. Downstream evolution of the boundary layer for a flap angle 12°. The dash line represents the normal distance from the wall where the velocity is 95% of the free stream. Turbulent boundary layer 1/7th power law also plotted (--) for reference at final location.

These inflection points move upward (i.e., away from the wall) as the downstream distance increases. At the last measured downstream location (x = 305 mm) the boundary layer has no inflection point.

3.2.2. Effect of the EAP Presence

When utilizing an installed flow control actuator it is important to quantify the effect that the presence of the actuator has on the flow field while not actuated. The EAP, although designed to be flat and integrated into the plate surface had some flaws. The surface of the EAP was compliant and inconsistent due to the adhesive holding the surface causing a slight surface roughness. Also, the material was loose on the surface so it was thought that a flow over it might cause some self-vibrations of the surface inducing disturbances to the flow. From observation of these imperfections it was clear that an experiment needed to be conducted that quantified the effect the unactuated EAP had on the flow. This case was used throughout the rest of the project as the "baseline" case (note that the data presented in Figures 10 to 14 were collected when a solid module was in place of the EAP).

Figure 15 shows the effects of the presence of EAP on the boundary layer development over the plate at a 12° flap deflection, and they are compared to the "clean" case where special SLA plugs were installed flush with the surface). Boundary layer profiles were acquired at 165, 190, 203, 216, 228, 241, and 254 mm downstream of the leading edge. It is clear that the boundary layer development is affected by the presence of the EAP for the majority of the plate. At x = 165 mm downstream from the leading edge the presence of the EAP yields a thicker boundary layer,
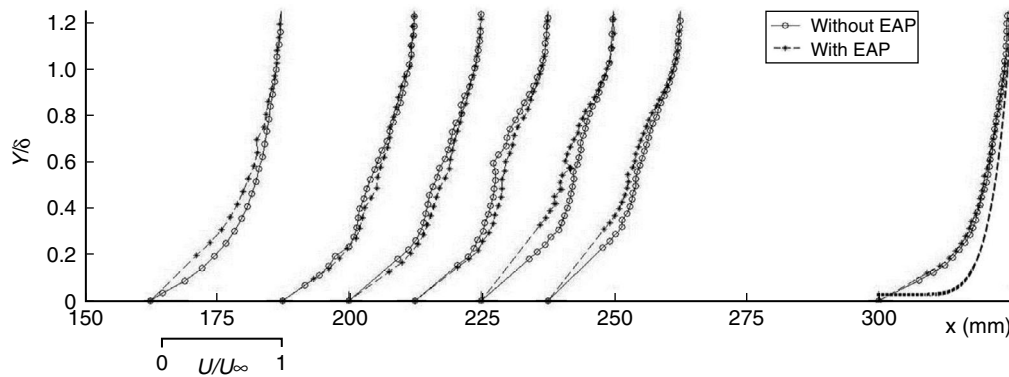
Figure 15. Normalized boundary layer profiles offset by different plate locations, with and without EAP installed and un-actuated. Turbulent boundary layer 1/7th power law also plotted (--) for reference at final location.

indicating that the transition process started closer to the leading edge (compared to the "clean" case). Farther downstream (x = 190 mm to 216 mm) the boundary layer is approximately the same, where both profiles contain inflection points at about the same cross-stream location. At x = 228 mm and 241 mm the boundary layer seems to be more affected by the EAP presence; however, it might be within error of the linear extrapolation process used for aligning the boundary layers (each boundary layer was measured as close to the surface as possible, and then linear extrapolation was used to find the point at which the velocity would be zero and that location was used as y = 0). Farther downstream, the boundary layers are almost identical, both turbulent as expected. This result indicates that although the presence of the unactuated EAP has some unintended effects, it can be assumed that the region of interest over the plate remains the same as the "clean" case, where the transition occurs between x = 178 mm to 254 mm.

3.2.3. EAP Actuation Effects

Next, the effect of the actuated EAP on the evolution of the boundary layer for the time averaged velocity and turbulent intensity was examined and it is presented in Figures 16a–c and 16d–f, respectively. The effect of actuating the EAP was examined at two actuation frequencies of 40 Hz and 500 Hz (corresponding to the TS wave and the KH wave associated with the inflection point in the velocity profile, respectively) at input voltage amplitude of 2000 V. The velocity and turbulent intensity profiles are presented at x = 203 mm, 241 mm, and 305 mm are presented in Figures 16a and d, 16b and e, and 16c and f, respectively, chosen due to the location of the inflection point. At x = 203 mm, actuating the EAP at a frequency of 500 Hz has the largest effect on the boundary layer, where it is being pulled closer to the surface, whereas actuation at a frequency of 40 Hz seems to have little to no effect at this streamwise location. Furthermore, the higher frequency actuation has a significant effect on the turbulence intensity distribution, where the maximum intensity is reduced and the cross-stream region of high intensity is increased. The peak turbulence intensities for the baseline and the 40 Hz cases are roughly 10%, and 8.6% for the 500 Hz case. Farther downstream (at x = 241 mm, Figures 16b and e) the baseline flow exhibits an inflection point, whereas when high frequency actuation is used the inflection point is mitigated. This suggests that the transition to a turbulent boundary layer is promoted. On the other hand, the low frequency actuation has little to no effect indicating that the TS waves are being dominated by the already transitioning flow. This could mean that in order for the TS waves to be more effectively amplified the EAP needs to be actuated farther upstream from the region of interest. This would give the excitation of the T-S waves more time to develop and alter the flow field. Moreover, the turbulence intensity profile is affected mainly by the 500 Hz actuation, where the peak is closer to the surface; however, for all three cases, the peak turbulent intensity is similar at roughly 12%. At the last measurement location (x = 305 mm, Figures 16c and f) the velocity profile of the baseline case resembles a turbulent profile, where the effect of actuation is significantly reduced, where the velocity gradient near the wall is increased and the peak turbulent intensity is slightly reduced.
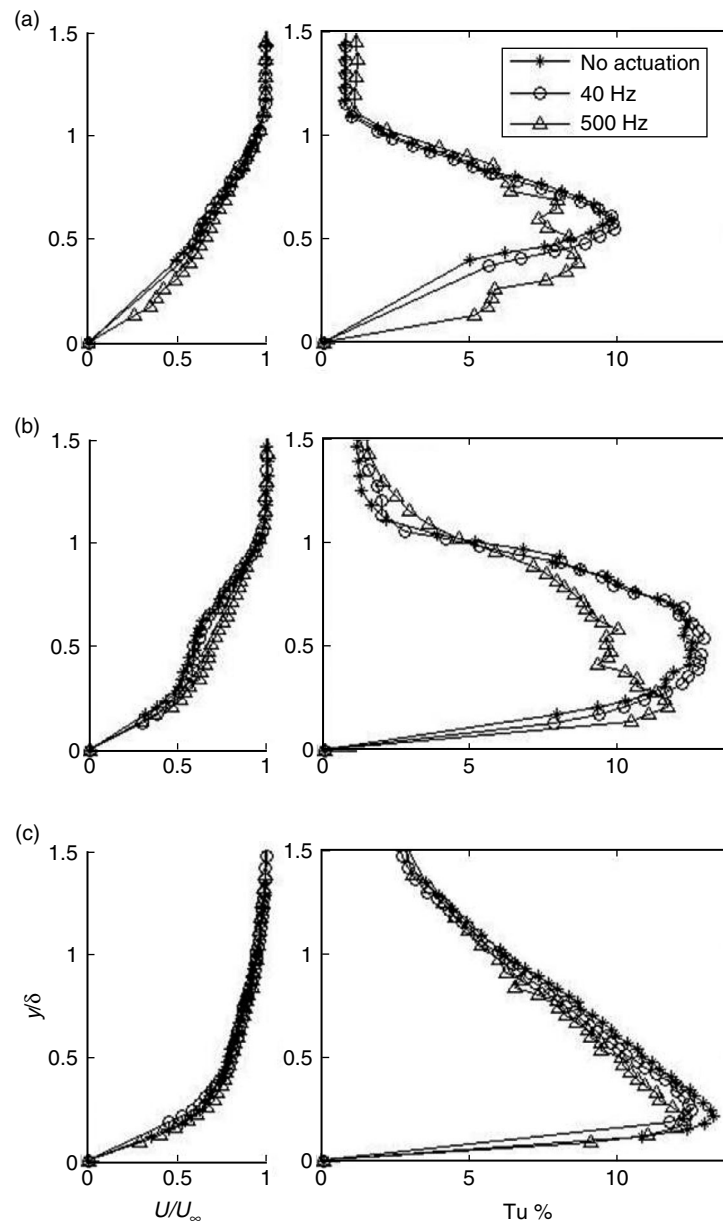
Figure 16. Normalized boundary layer profile and turbulence intensity for different actuation frequencies; x = (a) 203 mm, (b) 241 mm, and (c) 305 mm.

SUMMARY

The feasibility of using surface mounted electro active polymer (EAP) to alter the boundary layer over a flat plate was explored experimentally in a small-scale wind tunnel. First, the response of the EAP to different input voltages and driving frequencies was investigated experimentally using a Laser Displacement Velocimetry. It was found that the EAP deflected into the pocket in a parabolic manner, where the maximum deflection was obtained in the center of the EAP, where peak deflections of 0.25 mm and 0.35 mm were obtained for driving frequencies of 500 Hz and 40 Hz, respectively, at a input voltage amplitude of 2000 V.

The effects of the EAP on a flat plate boundary layer under an induced favorable pressure gradient was investigated using a single hotwire sensor, where the pressure gradient was varied using a small flap that was mounted at the trailing edge of the plate. Boundary layer measurements were taken as a baseline for two flap deflections of 0° and 12° to show the effect the flap has on the boundary layer shape and evolution. It was shown that deflecting the flap induced earlier transition to turbulence.

Two driving frequencies were chosen for the EAP actuation, a frequency of 40 Hz to excite the TS waves and a frequency of 500 Hz to excite the inflection point instability. The higher frequency proved to be much more affective at mitigating the inflection point in the boundary layer as well as shifting the peak turbulence intensity closer to the surface of the plate due to the fact that the inflection point instability is much more sensitive to control because it is inviscid. The frequency corresponding to the TS waves was found to be much less effective since the boundary layer was transitional at the location of the EAP.

The results presented in this paper show that EAP was successful in altering a boundary layer with a favorable pressure gradient, causing an early transition. This indicates that it might become a useful flow control device to manipulate boundary layers for transition and or separation control.

REFERENCES

[1]   Abdullah, E., Bil, C. and Watkins S., "Application of Smart Materials for Adaptive Airfoil Control", AIAA paper 2009–1359.

[2]   Amitay, M., Smith, D.R., Kibens, V., Parekh, D.E., and Glezer, A., "Aerodynamic Flow Control over Unconventional Airfoil Using Synthetic Jet Actuators", AIAA Journal, Vol. 39, No. 3, 2001, pp. 503–529.

[3]   Bastedo, W.G. and Mueller, T.J., "Spanwise Variation of Laminar Separation Bubbles on Wings at Low Reynolds Number", Journal of Aircraft, Vol. 23, No. 9, 1986, pp.687–694.

[4]   Betchov, R. and Szewczyk, A., "Stability of a shear layer between parallel streams", Physics of Fluids, Vol. 6, No. 10, 1963, pp.1391–1396.

[5]   Dearing, S., Lambert, S., Morrison, J., "Flow control with active dimples", The Aeronautical Journal, Paper No. 3174, 2007.

[6]   Diwan, S. and Ramesh, O., "Laminar separation bubbles: Dynamics and control", Sadhana, Vol. 32, No. 1–2, 2007, pp.103–109.

[7]   Ehlers, S.M. and Weisshaar, T.A., "Static Aeroelastic Control of an Adaptive Lifting Surface", Journal of Aircraft. Vol. 30, No. 4, 1993.

[8]   Gaster, M., "On the effects of boundary-layer growth on flow stability", Journal of Fluid Mechanics, Vol. 66, 1974, pp. 465–480.

[9]   Goksel, B., "Plasma Flow Control at MAV Reynolds Numbers", 3rd Us-European Competition and Workshop on Micro Air Vehicle Systems, 2007.

[10] Ifju, P.G., Jenkins D. A., Ettinger, S., Yongsheng, L., Shyy, W., and Waszak M.R., "Flexible-Wing-Based Micro Air Vehicle", AIAA Paper, 2002–0705.

[11] Lang, M., Rist, U. and Wagner, S., "Investigations on controlled transition development in a laminar separation bubble by means of LDA and PIV", Experiments in Fluids, Vol. 36, 2004, pp. 43–52.

[12] Lessen, M., "On stability of free laminar boundary layer between parallel streams", NACA Report 979, 1950.

[13] Lock, R.C., "The velocity distribution in the laminar boundary layer between parallel streams", Quart. J. Mech. Appl. Math., 4, 1951, pp. 42–62.

[14] Marxen, O., Lang, M., Rist, U., and Wagner, S., "A Combined Experimental/Numerical Study of Unsteady Phenomena in a Laminar Separation Bubble", Flow Turbulence and Combustion, Vol. 71, 2003, pp. 133–146.

[15] Marxen, O., Kotapati, R.B., and You, D., "Evaluation of active control of a laminar separation bubble based on linear stability theory", Center for Turbulence Research Annual Research Briefs, 2006, pp. 323–335.

[16] Mueller, T.J. and DeLaurier, J.D., "Aerodynamics of Small Vehicles", Annual Review of Fluid Mechanics.Vol. 35, 2003, pp. 89–111.

[17] Narasimha, R., and Prasad, S.N., "Leading edge shape for flat plate boundary layer studies", Experiments in Fluids, Vol. 17, No. 5, 1994, pp. 358–360.

[18] Pinkerton, J.L. and Moses, R. W., "A Feasibility Study to Control Airfoil Shape Using THUNDER", NASA Technical Memorandum, 4767, 1997.

[19] Schlichting, H., "Uber die Enstehung der Turbulenz bei der Plattenstromung", Math. Phys. Klasse, 1932, pp. 160–98.

[20] Schlichting, H., **Boundary-Layer Theory**, 7th Ed. The Mcgraw-Hill Book Company, Inc. Germany, 1979.

[21] Tollmien W., "Uber die Entsehung der Turbulenz", Math. Phys. Klasse, 1926, pp. 21–44.

[22] Udovidchik, N., Morrison, J.F., "Investigation of Active Dimple Actuators for Separation Control", AIAA Paper 2006–3190.

[23] Winklemann, A.E. and Barlow, J.B., "A Flowfield Model for a Rectangular Planform Wing", AIAA Journal, Vol. 18, Aug. 1980, pp. 1006–1008.